

Gradient flow running coupling in SU(2) with $N_f = 6$ flavors

Viljami Leino*

Helsinki Institute of Physics and Department of Physics, University of Helsinki

E-mail: viljami.leino@helsinki.fi

Teemu Rantalaiho

Helsinki Institute of Physics and Department of Physics, University of Helsinki

E-mail: teemu.rantalaiho@helsinki.fi

Kari Rummukainen

Helsinki Institute of Physics and Department of Physics, University of Helsinki

E-mail: kari.rummukainen@helsinki.fi

Joni M. Suorsa

Helsinki Institute of Physics and Department of Physics, University of Helsinki

E-mail: joni.suorsa@helsinki.fi

Kimmo Tuominen

Helsinki Institute of Physics and Department of Physics, University of Helsinki

E-mail: kimmo.i.tuominen@helsinki.fi

Sara Tähtinen

Helsinki Institute of Physics and Department of Physics, University of Helsinki

E-mail: sara.tahtinen@helsinki.fi

We present preliminary results of the running of the coupling in SU(2) gauge theory with 6 massless fundamental representation fermion flavors. We measure the coupling using the gradient flow method with Schrödinger functional boundary conditions. The results are consistent with perturbation theory in the weak coupling and we see an indication of infrared fixed point at strong coupling.

34th annual International Symposium on Lattice Field Theory

24-30 July 2016

University of Southampton, UK

*Speaker.

1. Introduction

Many phenomenologically viable models of beyond standard model physics can be built on asymptotically free gauge theories where the running of the coupling approaches a non-trivial infrared fixed point (IRFP) and the long distance physics becomes conformal. Given a $SU(N_c)$ gauge theory with N_f massless flavors of Dirac fermions, we can locate theories with an IRFP by choosing a fermion representation and varying the number of fermions N_f . The range of values N_f where the theory has an IRFP is called the conformal window. The upper edge of conformal window can be calculated from perturbation theory by finding the N_f where the one-loop coefficient of the β -function vanishes. Over this region the theory loses its asymptotic freedom. However, as the N_f is lowered, the IRFP will shift towards larger couplings until a spontaneous chiral symmetry breaking occurs and theory becomes QCD-like. The smallest N_f that still has a IRFP behavior marks the lower edge of the conformal window. This lower boundary is typically located at strong coupling, which mandates the use of nonperturbative methods, such as lattice simulations, to determine its location. Over recent years this question has been heavily studied in multiple different models.

In this paper we focus on $SU(2)$ gauge theory with six flavors of fundamental representation massless fermions. This theory is supposed to be near the lower edge of the conformal window, which is estimated to be between $N_f \sim 6 - 8$ by different approximations [1–3]. From previous lattice studies the $N_f = 4$ and $N_f = 8, 10$ cases are known to be outside and inside of the conformal window respectively [4–6]. Direct searches for the presence or the lack of an IRFP for the six fermion case have, however, been inconclusive [6–9].

We employ the the gradient flow finite volume method [10, 11], with Schrödinger functional boundary conditions [12, 13] to measure the running of the coupling constant. This allows us to reach vanishing fermion mass and measure the mass anomalous dimension alongside the coupling [14]. We run the analysis with multiple discretizations and find a clear indication of IRFP at $g_{GF}^2 \sim 13 - 15$.

2. Methods and Results

In this work we study the $SU(2)$ gauge theory with six massless Dirac fermions in the fundamental representation. We use the HEX smeared [15], clover improved Wilson fermion action with partially smeared plaquette gauge action as our lattice formulation:

$$S = (1 - c_g)S_G(U) + c_g S_G(V) + S_F(V) + c_{SW} \delta S_{SW}(V), \quad (2.1)$$

where V and U are the smeared and unsmeared gauge fields respectively. The smearing of the standard single plaquette Wilson gauge action S_G is tuned by the parameter c_g to remove the unphysical bulk phase transition from the region of interest in the parameter space [16]. Here we set $c_g = 0.5$. The clover Wilson fermion action S_F is non-perturbatively improved to order $\mathcal{O}(a)$ with the tree-level Sheikholeslami-Wohlert coefficient set to $c_{SW} \approx 1$.

We use the Schrödinger Functional method [12] with Dirichlet boundary conditions. On a lattice of size L^4 the gauge fields are set to unity and the fermion fields are set to zero at temporal

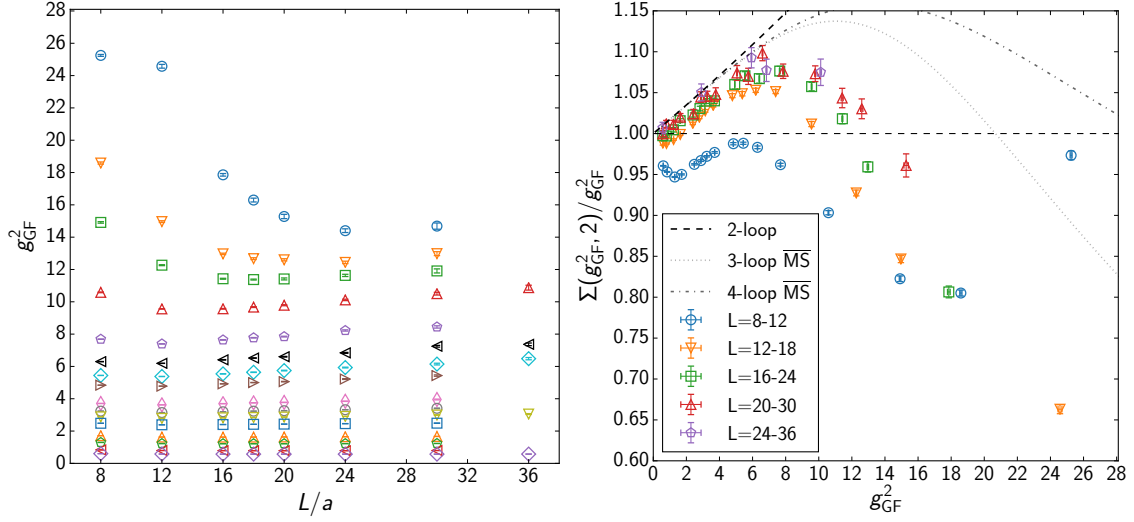


Figure 1: The plot on the left shows the gradient flow coupling (2.5) measured at each β and L/a at $c = 0.4$. The plot on the right shows the lattice step scaling function (2.7) for these couplings.

boundaries $x_0 = 0, L$:

$$\begin{aligned}
 U_k(0, \mathbf{x}) &= U_k(L, \mathbf{x}) = V_k(0, \mathbf{x}) = V_k(L, \mathbf{x}) = 1, \\
 U_\mu(x_0, \mathbf{x} + L\hat{\mathbf{k}}) &= U_\mu(x_0, \mathbf{x}), \quad V_\mu(x_0, \mathbf{x} + L\hat{\mathbf{k}}) = V_\mu(x_0, \mathbf{x}), \\
 \psi(0, \mathbf{x}) &= \psi(L, \mathbf{x}) = 0, \quad \psi(x_0, \mathbf{x} + L\hat{\mathbf{k}}) = \psi(x_0, \mathbf{x})
 \end{aligned}
 \tag{2.2}$$

where k labels one of the spatial directions. These boundary conditions enable us to both run simulations at vanishing quark mass, and measure the mass anomalous dimension alongside the running coupling.

We measure the running of the coupling using the Yang-Mills gradient flow. This method is set up by introducing a fictitious flow time t and studying the evolution of the flow gauge field $B_\mu(x, t)$ according to flow equation:

$$\partial_t B_\mu = D_\nu G_{\nu\mu}, \tag{2.3}$$

where $G_{\mu\nu}(x; t)$ is the field strength of the flow field B_μ and $D_\mu = \partial_\mu + [B_\mu, \cdot]$. The initial condition is defined such that $B_\mu(x; t=0) = A_\mu(x)$ in terms of the original continuum gauge field A_μ . In the lattice formulation the continuum flow field is replaced by the lattice link variable U , which is then evolved using either the tree-level improved Lüscher-Weisz pure gauge action (LW) [17] or the Wilson plaquette gauge action (W).

The flow smooths the gauge field over a radius $\sqrt{8t}$, removing the UV divergences and automatically renormalizing gauge invariant observables [10]. Thus we can use evolution of the field strength, to the leading order in perturbation theory in $\overline{\text{MS}}$ scheme, to define the coupling at scale $\mu = 1/\sqrt{8t}$ [11]:

$$\langle E(t) \rangle = \frac{1}{4} \langle G_{\mu\nu}(t) G_{\mu\nu}(t) \rangle = \frac{3(N^2 - 1)g_0^2}{128\pi^2 t^2} + \mathcal{O}(g_0^4), \tag{2.4}$$

$$g_{\text{GF}}^2(\mu) = \mathcal{N}^{-1} t^2 \langle E(t) \rangle|_{x_0=L/2, t=1/8\mu^2}, \tag{2.5}$$

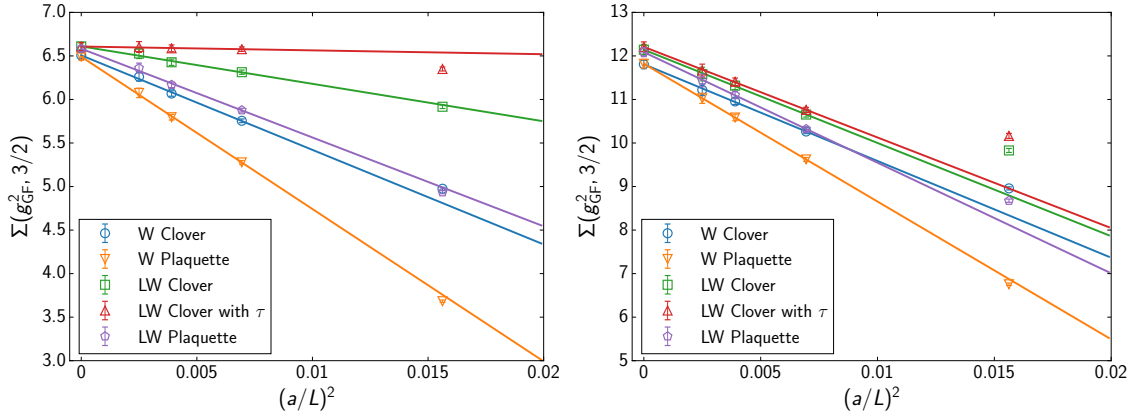


Figure 2: The continuum limit (2.8) with different discretizations and the effect of τ_0 -correction. Left: $g_{\text{GF}}^2 = 6$, Right: $g_{\text{GF}}^2 = 11$. The smallest lattice size is not used in the fit.

where the normalization factor \mathcal{N} has been calculated in [13] for the Schrödinger functional finite size scaling. As the translation symmetry is broken by the chosen boundary conditions, the coupling g_{GF}^2 is measured only on the central time slice $x_0 = L/2$. In the lattice formulation we measure the $\langle E(t) \rangle$ using both symmetric clover and simple plaquette discretizations.

In order to limit the scale into a regime $1/L \ll \mu \ll 1/a$, where (2.5) is free of both lattice artifacts and finite volume effects, we relate the lattice scale to the renormalization scale by defining a dimensionless parameter c_t as described in [18]:

$$\mu^{-1} = c_t L = \sqrt{8t}. \quad (2.6)$$

It is suggested in [13] that the SF scheme has reasonably small cutoff effects and statistical variance within the range of $c_t = 0.3 - 0.5$.

We choose to do bulk of our analysis with gradient flow evolved with Lüscher-Weisz action, clover definition of energy density (2.4), and $c_t = 0.3$. Results from these parameters can then be compared with the other discretizations to check the reliability of our analysis in the continuum limit. We run the simulations using lattice sizes 8, 12, 16, 18, 20, 24, 30 and 36 and with bare couplings within the range $g_0^2 \in [0.5, 8]$. The measured couplings with the aforementioned parameters are shown in figure 1. It is clear from the figure that the finite volume effects become substantial on smaller lattices as the coupling grows larger. Since the measurements on the $L = 36$ are incomplete, they will not be included in any advanced analysis.

To quantify the running of the coupling we use the finite lattice spacing step scaling function [19]:

$$\Sigma(u, L/a, s) = g_{\text{GF}}^2(g_0, sL/a) \Big|_{g_{\text{GF}}^2(g_0, L/a)=u}, \quad (2.7)$$

which describes the change of the measured coupling when the linear size of the system is increased from L to sL . Our data allows us to use either $s = 2$ or $s = 3/2$. For this paper we have chosen the step size $s = 3/2$. In figure 1 we show the scaled step scaling function $\Sigma(u, L/a, 3/2)/u$ calculated for the measured pairs 8 – 12, 12 – 18, 16 – 24, 20 – 30 and 24 – 36. The large coupling behavior of the 8 – 12 pair deviates significantly from the others probably due to finite volume effects.

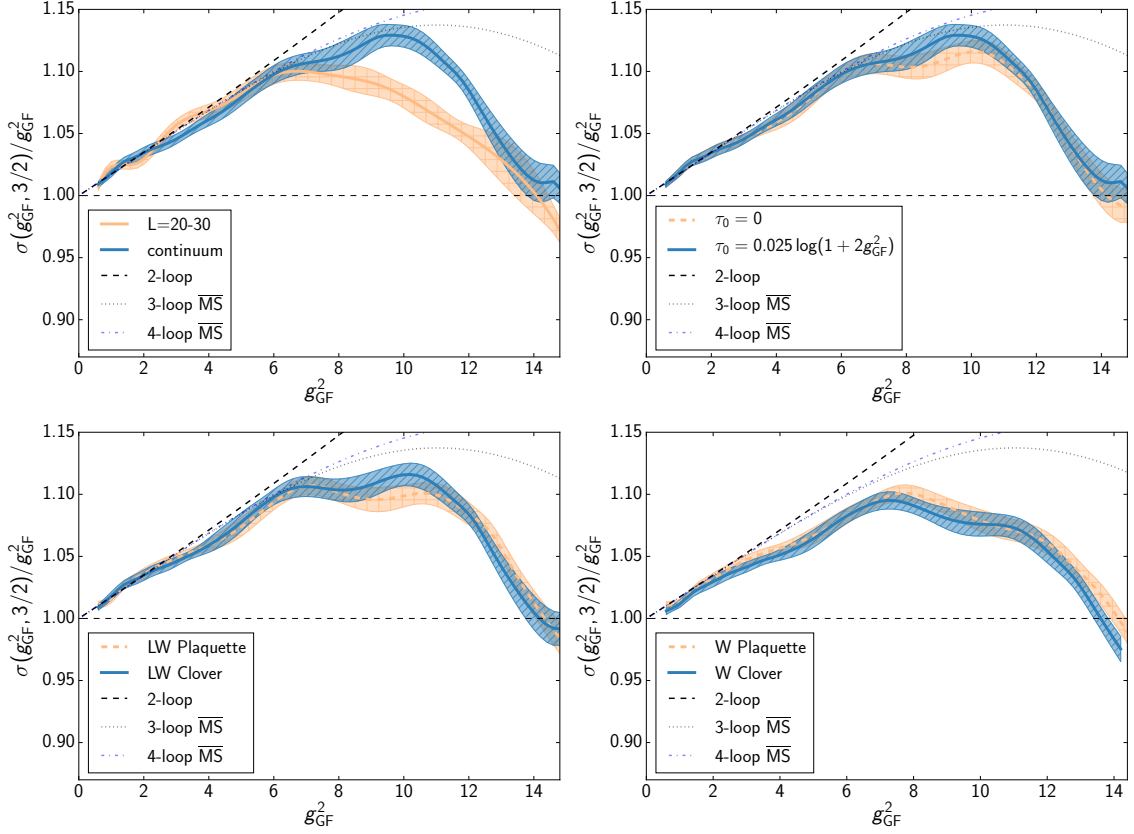


Figure 3: The scaled step scaling function with continuum extrapolation calculated and compared with different discretizations. Upper row: LW flow with clover energy with and without τ_0 correction. Lower row: Plaquette and clover E 's for LW and W evolved flows.

We expect the lowest order discretization effect to be of order $\mathcal{O}(a^2)$ and extrapolate the continuum limit of the step scaling function $\sigma(u)$ with a fit:

$$\Sigma(u, a/L) = \sigma(u) + c(u)(a/L)^2 \quad (2.8)$$

$$\sigma(u) = \lim_{a \rightarrow 0} \Sigma(u, a/L), \quad (2.9)$$

where we obtain the constant values of couplings at several lattice sizes by interpolating the measured couplings as:

$$\frac{g_{\text{GF}}^2(g_0)}{g_0^4} - \frac{1}{g_0^2} = \sum_{i=0}^m a_i g_0^{2i}, \quad m = 10. \quad (2.10)$$

With this choice of a polynomial function we achieve a combined $\chi^2/\text{d.o.f}$ of ~ 1.1 . We study the robustness of the fit by also running the interpolation with $m = 9$ and repeating the analysis.

The continuum limit of the step scaling function (2.8) can be used to give an estimate of the cutoff effects. As the gradient flow coupling is known to produce $\mathcal{O}(a^2)$ discretization effects we optimize the gradient flow coupling (2.5) to minimize the $\mathcal{O}(a^2)$ lattice artifacts in the continuum step scaling function by adding a tunable τ_0 correction to it, as suggested in [20]:

$$g_{\text{GF}}^2 = \frac{t^2}{\mathcal{N}} \langle E(t + \tau_0 a^2) \rangle = \frac{t^2}{\mathcal{N}} \langle E(t) \rangle + \frac{t^2}{\mathcal{N}} \langle \frac{\partial E(t)}{\partial t} \rangle \tau_0 a^2 + \mathcal{O}(a^4). \quad (2.11)$$

It turns out the precise value of τ_0 has a relatively small effect in the continuum extrapolation, as long as it is not allowed to grow too large [21]. For $c_t = 0.3$ a constant $\tau_0 = 0.05$ would suffice for most of the measured couplings, but it would be too large and affect the continuum limit for small couplings. Therefore we have decided to make the τ_0 -correction a function of the measured coupling g_{GF}^2 :

$$\tau_0 = 0.025 \log(1 + 2g_{\text{GF}}^2). \quad (2.12)$$

The measured coupling is used instead of the bare coupling in order to have a consistent $\mathcal{O}(a^2)$ shift in the step scaling analysis [22]. The final τ_0 is then calculated iteratively starting from $g_{\text{GF}}^2 = g_0^2$.

In figure 2 we show the a^2 -dependence of the step scaling function for all measured discretizations without any τ_0 correction compared to our chosen set of discretizations with the τ_0 correction (2.12) applied. τ_0 correction removes most of the $\mathcal{O}(a^2)$ cutoff effects in the small coupling regime where it was defined to do so. Generally the more improved discretizations (LW over W, clover over plaquette) seem to have smaller cutoff effects. However, we see clear violations on the leading $\mathcal{O}(a^2)$ scaling on small lattice sizes and therefore will not use smallest lattice size $L = 8$ in our analysis. Interestingly the Wilson flow with plaquette energy seems to have the most consistent $\mathcal{O}(a^2)$ scaling despite it having the largest cutoff effects.

We present the continuum extrapolations of step scaling function (2.9) for multiple different discretizations in the figure 3. Similar to lattice step scaling behavior in figure 1, the continuum step scaling follows the universal two loop perturbative curve closely up to $g_{\text{GF}}^2 \approx 7$ and then diverges towards an IRFP around $g_{\text{GF}}^2 \sim 14.5$. While the 3 and 4-loop $\overline{\text{MS}}$ curves are scheme dependent, and cannot be directly compared, they are shown as a reference. On the upper left picture where we have the continuum limit with the chosen set of discretizations and τ_0 -correction, we also show the lattice step scaling of the largest lattice pair $L = 20 - 30$. From the other pictures we can see all discretizations to mostly agree in the continuum within $1 - \sigma$ error bands.

3. Conclusions

We have studied the running coupling in the $SU(2)$ lattice gauge theory with 6 fermions in the fundamental representation. Gradient flow algorithm with Schrödinger functional boundaries gives us a clear look to large coupling behavior of this theory. We see a clear indication of a fixed point around $g_{\text{GF}}^2 \sim 13 - 15$ in the step scaling analysis. The continuum limit is robust regardless of the discretizations used. For added reliability, results with different c_t remain to be calculated. The results for the mass anomalous dimension are reported in [14].

4. Acknowledgments

This work is supported by the Academy of Finland grants 267842, 134018 and 267286, T.R. and S.T. are funded by the Magnus Ehrnrooth foundation and J.M.S. by the Jenny and Antti Wihuri foundation. The simulations were performed at the Finnish IT Center for Science (CSC) in Espoo, Finland. Parts of the simulation program have been derived from the MILC lattice simulation program [23].

References

- [1] F. Sannino and K. Tuominen, Phys. Rev. D **71**, 051901 (2005) doi:10.1103/PhysRevD.71.051901 [hep-ph/0405209].
- [2] D. D. Dietrich and F. Sannino, Phys. Rev. D **75**, 085018 (2007) doi:10.1103/PhysRevD.75.085018 [hep-ph/0611341].
- [3] M. T. Frandsen, T. Pickup and M. Teper, Phys. Lett. B **695**, 231 (2011) doi:10.1016/j.physletb.2010.10.064 [arXiv:1007.1614 [hep-ph]].
- [4] V. Leino, T. Karavirta, J. Rantaharju, T. Rantalaiho, K. Rummukainen, J. M. Suorsa and K. Tuominen, PoS LATTICE **2015**, 226 (2016) [arXiv:1511.03563 [hep-lat]].
- [5] H. Ohki, T. Aoyama, E. Itou, M. Kurachi, C.-J. D. Lin, H. Matsufuru, T. Onogi and E. Shintani *et al.*, PoS LATTICE **2010**, 066 (2010) [arXiv:1011.0373 [hep-lat]].
- [6] T. Karavirta, J. Rantaharju, K. Rummukainen and K. Tuominen, JHEP **1205** (2012) 003 [arXiv:1111.4104 [hep-lat]].
- [7] F. Bursa, L. Del Debbio, L. Keegan, C. Pica and T. Pickup, Phys. Lett. B **696** (2011) 374 [arXiv:1007.3067 [hep-ph]].
- [8] M. Hayakawa, K.-I. Ishikawa, S. Takeda, M. Tomii and N. Yamada, Phys. Rev. D **88** (2013) 9, 094506 [arXiv:1307.6696 [hep-lat]].
- [9] T. Appelquist, R. C. Brower, M. I. Buchoff, M. Cheng, G. T. Fleming, J. Kiskis, M. F. Lin and E. T. Neil *et al.*, Phys. Rev. Lett. **112** (2014) 111601 [arXiv:1311.4889 [hep-ph]].
- [10] M. Luscher and P. Weisz, JHEP **1102**, 051 (2011) [arXiv:1101.0963 [hep-th]].
- [11] M. Luscher, JHEP **1008**, 071 (2010) [arXiv:1006.4518 [hep-lat]].
- [12] M. Luscher, P. Weisz and U. Wolff, Nucl. Phys. B **359**, 221 (1991).
- [13] P. Fritzsche and A. Ramos, JHEP **1310**, 008 (2013) [arXiv:1301.4388 [hep-lat]].
- [14] J.M. Suorsa, V. Leino, J. Rantaharju, T. Rantalaiho, K. Rummukainen and K. Tuominen, These proceedings
- [15] S. Capitani, S. Durr and C. Hoelbling, JHEP **0611** (2006) 028 [hep-lat/0607006].
- [16] T. DeGrand, Y. Shamir and B. Svetitsky, PoS LATTICE **2011**, 060 (2011) [arXiv:1110.6845 [hep-lat]].
- [17] M. Luscher and P. Weisz, Commun. Math. Phys. **97**, 59 (1985) Erratum: [Commun. Math. Phys. **98**, 433 (1985)]. doi:10.1007/BF01206178
- [18] Z. Fodor, K. Holland, J. Kuti, D. Nogradi and C. H. Wong, JHEP **1211**, 007 (2012) doi:10.1007/JHEP11(2012)007 [arXiv:1208.1051 [hep-lat]].
- [19] M. Luscher, R. Sommer, P. Weisz and U. Wolff, Nucl. Phys. B **413**, 481 (1994) [hep-lat/9309005].
- [20] A. Cheng, A. Hasenfratz, Y. Liu, G. Petropoulos and D. Schaich, JHEP **1405**, 137 (2014) [arXiv:1404.0984 [hep-lat]].
- [21] A. Hasenfratz, D. Schaich and A. Veernala, JHEP **1506**, 143 (2015) doi:10.1007/JHEP06(2015)143 [arXiv:1410.5886 [hep-lat]].
- [22] A. Ramos, PoS LATTICE **2014**, 017 (2015) [arXiv:1506.00118 [hep-lat]].
- [23] <http://physics.utah.edu/~detar/milc.html>